PHARMACIA

Pharmacia 72: 1–14
DOI 10.3897/pharmacia.72.e139559

Research Article

Computational insights into Sitahe (*Leuconotis eugenifolia*) bioactive compounds: A promising approach for radioprotection through p53 inhibition

Dian Pribadi Perkasa[1], Iin Kurnia[2,3], Taufik Muhammad Fakih[4,5], Teja Kisnanto[2], Dwi Ramadhani[2], Harry Nugroho Eko Surniyantoro[2], Boky Jeanne Tuasikal[1], Alfian Mahardika Forentin[2], Mukh Syaifudin[2,3]

1 *Research Center for Radiation Process Technology, Research Organization for Nuclear Energy, National Research and Innovation Agency (BRIN), Building 71, Kawasan Puspiptek, Setu, Tangerang Selatan, Banten 15310, Indonesia*

2 *Research Center for Radioisotope, Radiopharmaceutical and Biodosimetry Technology, Research Organization for Nuclear Energy, National Research and Innovation Agency (BRIN), Building 71, Kawasan Puspiptek, Setu, Tangerang Selatan, Banten 15310, Indonesia*

3 *Research Collaboration Center for Theranostic Radiopharmaceuticals, National Research and Innovation Agency (BRIN), Jl. Raya Bandung Sumedang KM 21, Sumedang, West Jawa, 45363, Indonesia*

4 *Department of Pharmacy, Faculty of Mathematics and Natural Sciences, Universitas Islam Bandung, Jl. Ranggagading, Bandung, West Java, 40116, Indonesia*

5 *Department of Pharmaceutical Analysis and Medicinal Chemistry, Faculty of Pharmacy, Universitas Padjadjaran, Jl. Raya Bandung Sumedang KM 21, Sumedang, West Java, 45363, Indonesia*

Corresponding author: Mukh Syaifudin (mukh002@brin.go.id)

Received 17 October 2024 ♦ **Accepted** 6 December 2024 ♦ **Published** 16 January 2025

Citation: Perkasa DP, Kurnia I, Fakih TM, Kisnanto T, Ramadhani D, Surniyantoro HNE, Tuasikal BJ, Forentin AM, Syaifudin M (2025) Computational insights into Sitahe (*Leuconotis eugenifolia*) bioactive compounds: A promising approach for radioprotection through p53 inhibition. Pharmacia 72: 1–14. https://doi.org/10.3897/pharmacia.72.e139559

Abstract

The radioprotective potential of Sitahe (*Leuconotis eugenifolia*) phytochemicals in cancer radiotherapy remains largely unexplored. In this study, in silico docking simulations were conducted to systematically assess the ability of key phytochemicals from Sitahe to modulate p53 activity, a critical gene in DNA repair and cancer therapy. SwissADME analysis revealed favorable physicochemical properties for compounds such as baurenol, alpha amyrin, and beta amyrin, although high lipophilicity may pose challenges for bioavailability. Molecular docking studies identified strong binding affinities between these compounds and the p53 DNA binding domain, with baurenol demonstrating the highest binding affinity at −6.75 kcal/mol, which is better compared to rhazinilam (−4.55 kcal/mol), leuconolam (−4.36 kcal/mol), leuconoxine (−4.26 kcal/mol), and dehydroleuconoxine (−4.76 kcal/mol). Hydrogen bonding with key residues such as Thr123 further enhanced the stability of these complexes. The low inhibition constants (Ki) suggest significant inhibitory potential, particularly for baurenol (11.31 μM). To evaluate the stability and reliability of these interactions, molecular dynamics (MD) simulations were performed over a duration of 500 ns. The results demonstrated that the selected compounds maintained stable molecular dynamics profiles, showing consistent interactions with the target protein throughout the simulation period. Among the compounds tested, baurenol exhibited the best performance with a MM/PBSA binding energy of −68.568 kJ/mol, which is better than rhazinilam (−63.538 kJ/mol). These findings suggest that baurenol, along with other Sitahe phytochemicals, could serve as dual-function agents, offering protection to healthy tissues from radiation-induced damage while targeting cancer cells through p53 modulation. Although these in silico and MD results are promising, further validation through in vitro and in vivo studies is essential to confirm their therapeutic potential and optimize their pharmacokinetic properties. This study positions Sitahe phytochemicals, particularly baurenol, as promising candidates for the development of novel radioprotective agents in cancer treatment.

Keywords

Sitahe bioactive compounds, radioprotective agents, p53 modulation, molecular modeling simulations, phytochemicals in cancer therapy

Introduction

Cancer is a disease characterized by the uncontrolled and abnormal growth of cells. These cells bypass the body's regulatory systems, leading to continuous and unchecked division (Street 2019). The disease originates from accumulated genetic and epigenetic changes that disrupt the normal mechanisms of cell regulation. Cancer cells not only proliferate uncontrollably, but they also invade nearby tissues and metastasize to distant organs. Genetic mutations further increase the aggressiveness of these cells, promoting their spread. As they replicate, cancer cells form clones and detach from their original site, traveling through the body to colonize new areas (Farshchi and Hasanzadeh 2023). To support their survival and growth, these cells activate autophagy and suppress apoptosis, allowing them to avoid programmed cell death. This resistance to apoptosis is often caused by alterations in signaling pathways, such as Bcl-2 overexpression and p53 mutations (Irish et al. 2007; Ameh-Mensah et al. 2021). Cancer is typically treated with external beam radiotherapy, which targets and destroys malignant cells. However, the complexity of the disease makes treatment challenging, as cancer cells can adapt and resist therapeutic interventions.

Radiotherapy involves the use of high-energy radiation to damage the DNA of cancer cells, leading to their destruction through apoptosis. It is often applied either as a standalone treatment or in conjunction with other therapeutic approaches, particularly after surgery, to eradicate any residual cancerous cells (Gong et al. 2021). A variety of critical factors, including tumor type, size, inherent sensitivity to radiation, and the condition of adjacent healthy tissues, play a significant role in treatment outcomes. The variability in responses among cancer cells, due to their heterogeneity, makes predicting outcomes more complex (Man et al. 2023). Moreover, ionizing radiation not only targets cancer cells but also inadvertently affects normal cells in the vicinity, causing potential harm to healthy tissue. Minimizing these adverse effects is essential for improving the quality of life of patients undergoing treatment. To safeguard healthy cells without compromising the efficacy of radiotherapy on cancer cells, it is essential to develop safe and selective radioprotective agents (Chen and Kuo 2017; Vinod and Hau 2020). These agents should shield healthy tissue without diminishing the treatment's ability to kill cancerous cells.

Phytochemicals derived from plants have gained significant recognition as potential candidates for drug development, particularly in cancer treatment. These compounds exhibit notable anticarcinogenic and antimutagenic properties, as demonstrated in various studies using cell lines and animal models. Sitahe (*Leuconotis eugenifolia*), a plant native to Aceh, Indonesia, and Malaysia, is traditionally consumed for its stamina-enhancing and medicinal benefits (Praptiwi et al. 2020). The phytochemicals in Sitahe, including alkaloids, flavonoids, steroids, and phenolics, have shown potent antimicrobial and antioxidant effects. Sitahe extracts are rich in bioactive compounds like baurenol, alpha amyrin, and beta amyrin, which may provide therapeutic benefits. Studies suggest that these compounds could be useful in preventing oxidative stress and microbial infections (Villaseñor et al. 2004; Choi et al. 2020). The discovery of such properties encourages further investigation into the plant's potential for disease treatment. By leveraging these phytochemicals, Sitahe presents a promising avenue for developing new therapeutic agents.

The leaves of Sitahe contain several bioactive compounds, including rhazinilam, leuconolam, leuconoxine, and dehydroleuconoxine (Sim et al. 1971). These compounds are traditionally used in medicine to treat digestive and liver issues. Rhazinilam has demonstrated anticancer, antibacterial, and anti-inflammatory properties, proving cytotoxic to cancer cell lines at low micromolar concentrations (Sirindil et al. 2022). Additionally, Leuconolam and its derivatives have been shown to possess strong antibacterial and antioxidant properties (Xu et al. 2013). Baurenol and beta amyrin have been identified for their ability to activate the p38 MAP kinase pathway, inducing cell death in Hela cells through the production of reactive oxygen species (ROS). Furthermore, alpha and beta amyrin have shown potential as inhibitors of proteins like ESR1, MAP2K2, and PGR, which play significant roles in cancer progression (Boller et al. 2010; Rehan and Shafiullah 2021). These findings highlight the therapeutic potential of Sitahe phytochemicals for future drug development.

The p53 gene plays a pivotal role in managing cell cycle regulation, especially in detecting DNA damage, initiating repair processes, and inducing apoptosis. p53 triggers cell death by activating pro-apoptotic genes like Bax, which, in turn, stimulates ICE protease, leading to protein degradation and subsequent DNA fragmentation (Bourdon et al. 2005; Yoon et al. 2009). Additionally, it promotes apoptosis through the activation of genes like PUMA and NOXA while simultaneously inhibiting anti-apoptotic genes by downregulating proteins like Bcl-2 and Bcl-xl. A loss of p53 function, whether due to mutation or other mechanisms, severely compromises genomic stability and fosters tumorigenesis (Nakano and Vousden 2001). Many cancer cells fail to express functional p53 and instead contain its mutated version, which contributes to more aggressive

and rapidly metastasizing tumors (Kobayashi et al. 2017). This malfunction results in impaired DNA replication and enhanced cancer progression.

Protein p53 is essentially a tumor suppressor and a transcription factor that regulates a multitude of genes involved in preventing tumor growth. However, its function can be inhibited by overexpression of MDM2, a known repressor of p53 (Bazanov et al. 2022). Recent research has shed light on several mechanisms governing p53-dependent transcriptional regulation, including the functional distinctions of its N-terminal transactivation domains, the diverse roles of its C-terminal domain, and its capacity to recognize enhancers across various chromatin landscapes. Furthermore, context-dependent mechanisms can fine-tune the p53 transcriptional program (Pereira et al. 2019; Koo et al. 2022). Inhibiting p53 activity can also be achieved through natural bioactive molecules found in compounds like Sitahe, which may offer multitarget therapy, as shown in Fig. 1.

The use of in silico techniques involving computational models and simulations has proven to be an effective approach in modern drug discovery. These methods rely on validated protocols to accurately predict the interactions between ligand molecules and their target receptors. In addition, in silico studies are instrumental in identifying natural compounds that could bind with target proteins, enhancing the drug development process. Computer-aided drug design (CADD) significantly contributes to pharmaceutical research by estimating the therapeutic potential of compounds in silico, thus supporting subsequent in vitro and in vivo experiments (Chua et al. 2023; Shareef et al. 2024). This research specifically examined the interaction between Sitahe's secondary metabolites and the proapoptotic protein p53, involving a series of processes such as ligand preparation, optimization, and validation. Simulations were performed to analyze ligand-protein binding affinities, while the ADMET (absorption, distribution, metabolism, excretion, and toxicity) profiles were predicted under the assumption that the ligand maintains flexibility while the protein remains rigid.

Materials and methods

Ligand preparation

The chemical compositions of Sitahe (*Leuconotis eugenifolia*) were gathered from various scholarly sources for this investigation (Fig. 2). MarvinSketch software was employed to confirm the chemical structures of the relevant compounds. The three-dimensional models of these compounds were constructed using PyMOL 1.3 (Delano 2002). For energy minimization, Gabedit 2.5.0 was applied to optimize the molecular configurations (Allouche 2012). To assess the bioactivity of these compounds, SwissADME (https://www.swissadme.ch/), an online prediction tool, was utilized (Daina et al. 2017). These platforms provided insights into the drug-like properties and the potential acute toxicity of the compounds under study.

Protein preparation

Based on previous research and the macromolecule structures available in the Protein Data Bank (PDB), the potential binding sites for interacting with p53 were identified, labeled under PDB ID: 6ZNC. These binding models were selected for further docking studies, with a resolution of 1.64 Å to ensure accuracy (Degtjarik et al. 2021). The protein structure was prepared using the Autodock Tools (ADT) 4.2.6 software, which helped define the ionization states and tautomeric forms of the amino acid residues (Forli et al. 2012). In this process, water molecules were removed, polar hydrogen atoms were added, and the Kollman-united atom partial charges and solvation parameters were assigned. The final protein configuration was saved in PDBQT file format, which is compatible with AutoGrid and AutoDock for molecular docking simulations.

Molecular docking

A workstation Dell equipped with an Intel Core i5-11400 CPU (12 MB cache, up to 4.40 GHz) and an NVIDIA Ge-

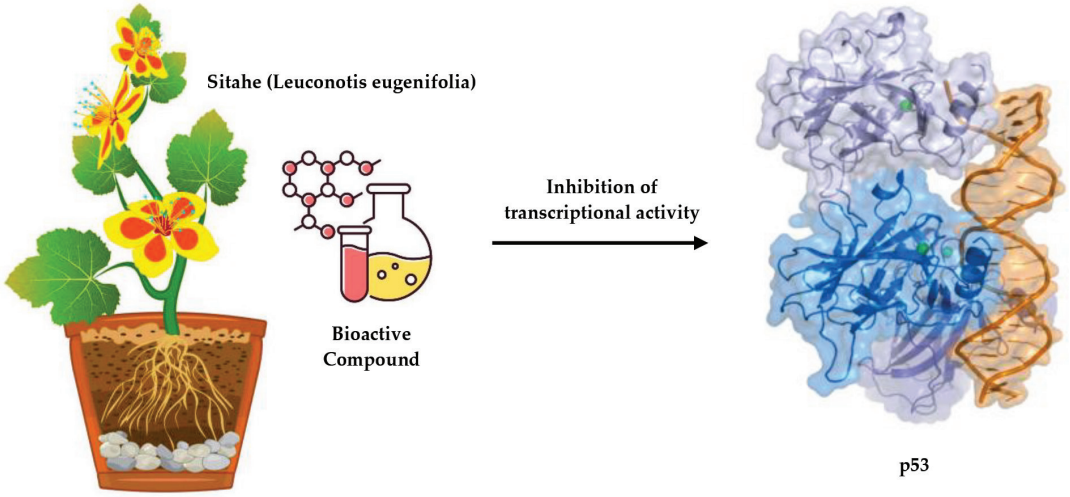

Figure 1. The inhibition of p53 activity can also be achieved through various bioactive molecules in Sitahe.

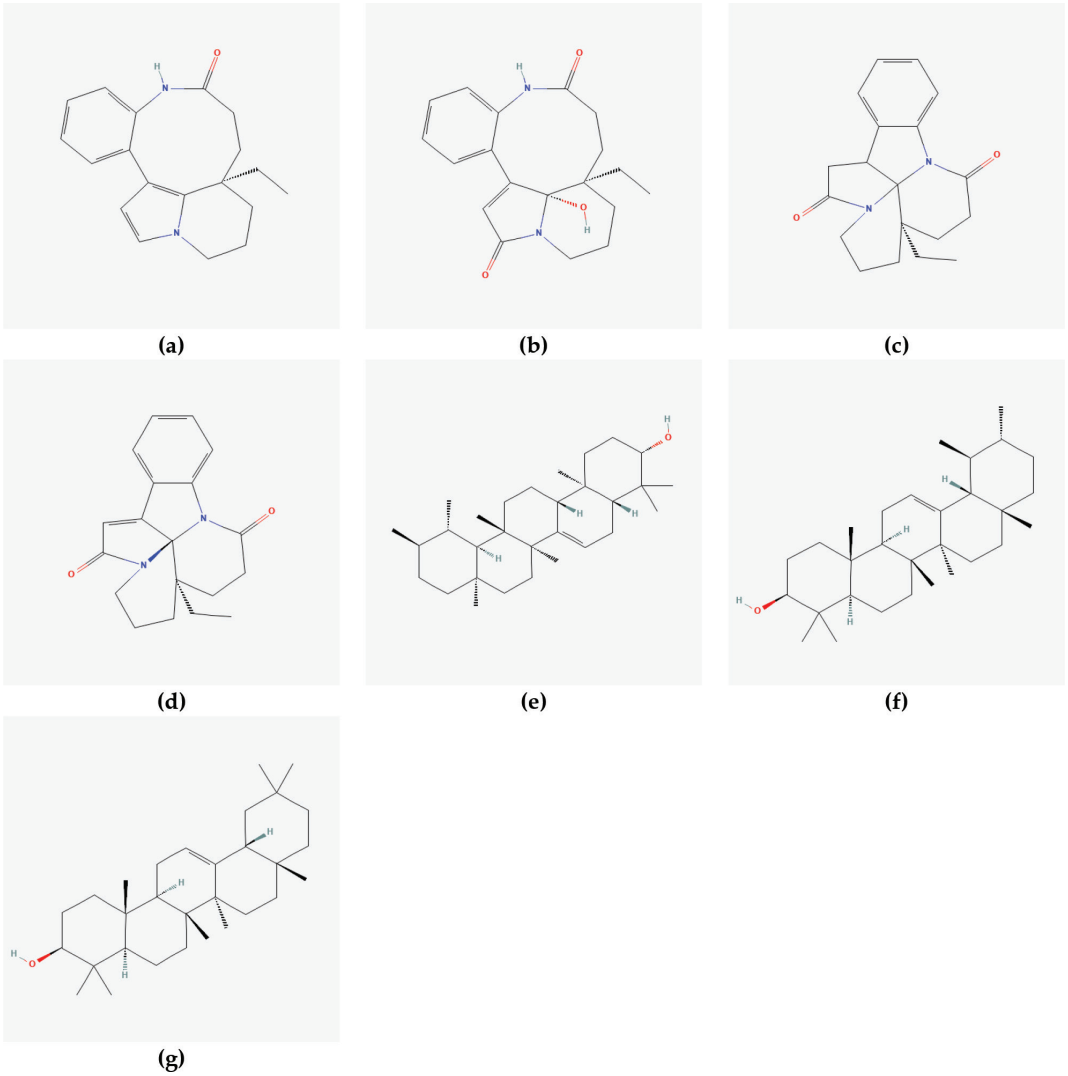

Figure 2. The 2D structures of the compounds. **a.** Rhazinilam; **b.** Leuconolam; **c.** Leuconoxine; **d.** Dehydroleuconoxine; **e.** Baurenol; **f.** Alpha amyrin, and **g.** Beta amyrin.

Force GTX 1080 Ti graphics card was employed to carry out the docking simulations. This system featured 64 GB of RAM, a 256 GB SATA HDD, and a 256 GB NVME SSD for efficient processing. Six software tools, including PyMOL 1.3, Discovery Studio Visualizer 2019 Client, LigPlus, Maestro, Gromacs 2016.3, and Visual Molecular Dynamics (VMD) 1.9.3, were utilized to evaluate and analyze the docking results, specifically focusing on the distances between hydrogen bonds and their binding partners. The docking and compilation of AutoDock 4.2.6 were performed on an Ubuntu 16.04.7 LTS (Xenial Xerus) operating system. AutoGrid and Autodock Tools (ADT) 4.2.6 were employed for calculating binding affinities for different ligand atom types and conducting molecular docking simulations. The Lamarckian Genetic Algorithm (LGA) was configured with the following parameters: 100 runs, elitism set to 1, a mutation rate of 0.02, a population size of 300, a crossover rate of 0.80, 27,000 generations, and 50,000,000 energy evaluations. The root-mean-square (RMS) cluster tolerance was set to 2.0 Å in each run. The ligand conformations chosen for further analysis were those that exhibited the lowest free binding energy from the most favorable cluster.

ADME prediction

The compounds were further evaluated for their ADME (Absorption, Distribution, Metabolism, and Excretion) characteristics using SwissADME integrated into Maestro software, with the analysis conducted in fast mode to expedite the prediction process. This approach aimed to efficiently assess how the compounds would behave pharmacokinetically within biological systems, providing insights into their potential suitability as drug candidates.

MD Simulations and Post-MD MM-PBSA

Molecular dynamics (MD) simulations were performed on the Gromacs 2016.3 platform for both the top ligand, baurenol, and the native ligand, rhazinilam, based on the docking results (Abraham et al. 2015a, 2015b, 2015c). The system was prepared by embedding the ligand-p53 complexes into TIP3P water molecules within a $10 \times 10 \times 10$ Å orthorhombic box. To neutralize the system, Na+ and Cl– ions were added, matching physiological ion concentrations. The SHAKE algorithm was used to constrain the movements of hydrogen

atoms within the system (Miyamoto and Kollman 1992). Following this, energy minimization was conducted using the OPLS4 force field, and the system was equilibrated with the NVT (isothermal–isochoric) and NPT (isothermal–isobaric) ensembles (Lu et al. 2021). The actual simulation was carried out for 500 ns, with snapshots taken every 100 ps, maintaining a constant 300 K temperature and 1 bar pressure. The Particle Mesh Ewald (PME) approach was used to manage long-range electrostatic interactions, with a 9.0 Å threshold for Coulomb interactions. Water molecules were modeled using the simple point charge (SPC) model, and the Nose–Hoover chain thermostat along with the Martyna–Tobias–Klein barostat were used for temperature and pressure control, respectively (Rühle 2007; Rogge et al. 2015). Throughout the simulation, a total of 50000 frames were recorded, which were later analyzed using the XMGrace tool. To further verify the docking results, the MM-PBSA method was employed to calculate the free binding energy of the three ligands using the trajectories of the p53–ligand complexes (Kumari et al. 2014; Wang et al. 2018). This was done through Schrödinger's Prime module, which utilizes the OPLS4 force field and the VSGB solvent model, along with rotamer search algorithms. Given the high computational demand, 500 frames were selected from the trajectory, with 1 frame taken every 100 frames to compute the free binding energies.

Results

Phytochemical library collection

Phytochemical compounds were extracted from Sitahe (*Leuconotis eugenifolia*), a plant species recognized for its medicinal potential. The identified compounds, including rhazinilam, leuconolam, leuconoxine, dehydroleuconoxine, baurenol, alpha amyrin, and beta amyrin, were sourced from previous studies. These phytochemicals were selected based on their documented biological activities and their availability in the PubChem database. Each compound was represented by its PubChem CID, a unique identifier used in computational studies (Table 1) (Kim et al. 2023). The selection was driven by the structural diversity of these compounds, offering a wide range of molecular interactions for computational evaluation. The choice of Sitahe as a phytochemical source was also influenced by its traditional use in herbal medicine, further motivating its exploration for pharmaceutical applications. The library of compounds was curated meticulously to ensure diversity in molecular weight, polarity, and other key physicochemical properties. Each phytochemical's molecular structure was visualized and retrieved in 2D format, preparing them for subsequent computational analyses (Fig. 2). This initial step laid the foundation for docking studies, molecular dynamics simulations, and ADME predictions.

Table 1. A library of various phytochemicals derived from Sitahe.

Phytochemical	Pubchem CID	Reference
Rhazinilam	11212435	(Goh et al. 1989; Gan et al. 2013; García-Ramírez et al. 2022)
Leuconolam	14442600	(Yang et al. 2014; Li et al. 2015; Geng et al. 2016)
Leuconoxine	70698272	(Geng et al. 2016; Pfaffenbach and Gaich 2017; Kim et al. 2019)
Dehydroleuconoxine	134949938	(Low et al. 2014)
Baurenol	111220	(Villaseñor et al. 2004; Boller et al. 2010; Choi et al. 2020)
Alpha amyrin	73170	(Nogueira et al. 2019; Viet et al. 2021; Chung et al. 2023)
Beta amyrin	73145	(Nogueira et al. 2019; Viet et al. 2021; Du et al. 2022)

Molecular docking

Based on the docking parameters presented in Table 2 and the corresponding 3D interactions of the selected phytochemicals from Sitahe with the p53 binding site, we can draw several conclusions regarding their potential as anticancer agents. In this study, the molecular docking of compounds such as rhazinilam, leuconolam, leuconoxine, dehydroleuconoxine, baurenol, alpha amyrin, and beta amyrin against the p53 binding site was carried out to evaluate their binding affinities and possible inhibitory effects. The docking scores, which ranged from −4.26 kcal/mol to −6.75 kcal/mol, demonstrate the compounds' potential to interact with the p53 protein. Baurenol displayed the strongest binding affinity with −6.75 kcal/mol, suggesting that it may have the most potent inhibitory action among the compounds studied. Meanwhile, alpha amyrin and beta amyrin also exhibited significant binding affinities of −6.15 kcal/mol and −6.04 kcal/mol, respectively, which further supports their potential as effective inhibitors.

Incorporating hydrogen bonding, the interaction between the ligand and protein plays a pivotal role. Hydrogen bonds, particularly with residues like Thr123 and Ser121, are key in stabilizing the ligand-protein complex. While most compounds formed hydrogen bonds with Thr123,

Table 2. Docking parameters for the phytochemicals derived from Sitahe.

Phytochemicals	Number of Heavy Atom(s)	Binding Affinity (kcal/mol)	Ligand Efficiency	KI (μM)	Number(s) of Hydrogen Bonding	Number(s) of Covalent Bonding
Rhazinilam	22	−4.55	0.21	462.15	0	1 with Cys124
Leuconolam	24	−4.36	0.18	638.22	2 with Thr123	0
Leuconoxine	23	−4.26	0.19	752.94	1 with Thr123	0
Dehydroleuconoxine	23	−4.76	0.21	326.56	2 with Thr123	0
Baurenol	31	−6.75	0.22	11.31	2 with Thr123	0
Alpha amyrin	31	−6.15	0.20	31.25	2 with Thr123	0
Beta amyrin	31	−6.04	0.19	37.38	1 with Ser121	0

alpha amyrin and beta amyrin exhibited two hydrogen bonds with this residue, contributing to binding stability. Similarly, baurenol demonstrated comparable interactions, underscoring its potential to modulate p53 function effectively. Notably, no covalent bond was formed between baurenol and p53, unlike the native ligand (rhazinilam), which forms a covalent bond with Cys124. Instead, baurenol relies on hydrogen bonding and hydrophobic interactions to stabilize its binding within the protein's active site. The 3D interaction diagrams illustrate these interactions within the hydrophobic binding pocket of p53 (Fig. 3). The hydrophobicity scale highlights the nonpolar regions of the binding pocket, where compounds like baurenol exhibit substantial contact, enhancing the overall binding strength through hydrophobic interactions and hydrogen bonding. These non-covalent interactions play a significant role in baurenol's ability to potentially modulate p53 function effectively without forming a covalent bond like the native ligand (Chen et al. 2021).

Given the results of this docking study, it is evident that the phytochemicals from Sitahe demonstrate promising potential as p53 modulators. However, further validation through molecular dynamics simulations and in vitro experiments is necessary to confirm the stability and efficacy of these interactions in a biological setting. These studies will provide valuable insights into how these compounds interact with p53 and their potential to alter its function in cancer cells. Additionally, exploring the pharmacokinetics and bioavailability of these phytochemicals will be crucial to assessing their practicality as therapeutic agents. These findings lay the groundwork for future research into the therapeutic potential of Sitahe phytochemicals in targeting p53 pathways, which are critical in the regulation of cancer cell proliferation and apoptosis.

ADME prediction

The physicochemical properties of the Sitahe phytochemicals presented in Table 3 offer insights into their potential as orally bioavailable compounds. The molecular weights (MW) of the compounds fall below the threshold of 500 g/mol, which is favorable for drug development in line with Lipinski's Rule of Five (Ro5) (Karami et al. 2022). However, baurenol, alpha amyrin, and beta amyrin exhibit molecular weights on the higher end (426.72 g/mol), yet still within acceptable limits for drug-likeness. The XLOGP3 Log P values show that most compounds have a high partition coefficient, particularly baurenol (9.01) and the amyrins (9.01 and 9.15). These values suggest strong lipophilicity, which aids in membrane permeability but may limit aqueous solubility. This is further reflected in the ESOL Log S values, with low solubility scores, particularly for baurenol (−8.16) and the amyrins (−8.16 and −8.25), indicating that solubility could be a challenge for these compounds in a pharmaceutical context.

In terms of TPSA (topological polar surface area), leuconolam shows the highest value (69.64 Å²), which is still within the optimal range for oral drugs, indicating good potential for hydrogen bonding and solubility. However, baurenol, alpha amyrin, and beta amyrin have low TPSA values (20.23 Å²), suggesting they are more lipophilic and may have limited interaction with aqueous environments but potentially better membrane permeability. The Csp3 fraction, which is a measure of the carbon atom hybridization in the molecule, is relatively high for baurenol and the amyrins (0.93), implying these compounds have a more 3D structure, potentially aiding in effective drug-receptor interactions. The number of rotatable bonds is generally low for all compounds, indicating a rigid structure, which often correlates with good oral bioavailability since it limits the flexibility of the molecule, potentially aiding in better receptor binding and fewer conformational changes (Krishnaiah 2010). These properties collectively suggest that while baurenol, alpha amyrin, and beta amyrin exhibit promising characteristics for permeability and interaction with biological membranes, their solubility could pose a challenge, and this aspect would need to be addressed in future drug formulation strategies.

MD simulations

To evaluate the behavior of baurenol and rhazinilam ligands with favorable docking scores, a molecular dynamics (MD) simulation was conducted for 500 ns using Gromacs 2016.3 software. The simulation utilized an explicit water model (TIP3P) to ensure realistic interactions between the ligands and the p53 protein (PDB: 6ZNC). MD simulations provide valuable insights into the flexibility, stability, and reliability of ligand binding modes within protein-ligand complexes. To assess the stability of these complexes, a root-mean-square deviation (RMSD) analysis was performed, as depicted in the

Table 3. Physicochemical properties of Sitahe phytochemicals for optimized oral bioavailability.

Phytochemicals	Physicochemical Feature					
	MW (g/mol)	XLOGP3 Log $P_{o/w}$	TPSA (A²)	ESOL Log S	Fraction Csp3	Rotatable Bond
Rhazinilam	294.39	2.94	34.03	−3.82	0.42	1
Leuconolam	326.39	1.01	69.64	−2.62	0.47	1
Leuconoxine	310.39	1.86	40.62	−3.06	0.58	1
Dehydroleuconoxine	308.37	1.65	40.62	−2.92	0.47	1
Baurenol	426.72	9.01	20.23	−8.16	0.93	0
Alpha amyrin	426.72	9.01	20.23	−8.16	0.93	0
Beta amyrin	426.72	9.15	20.23	−8.25	0.93	0

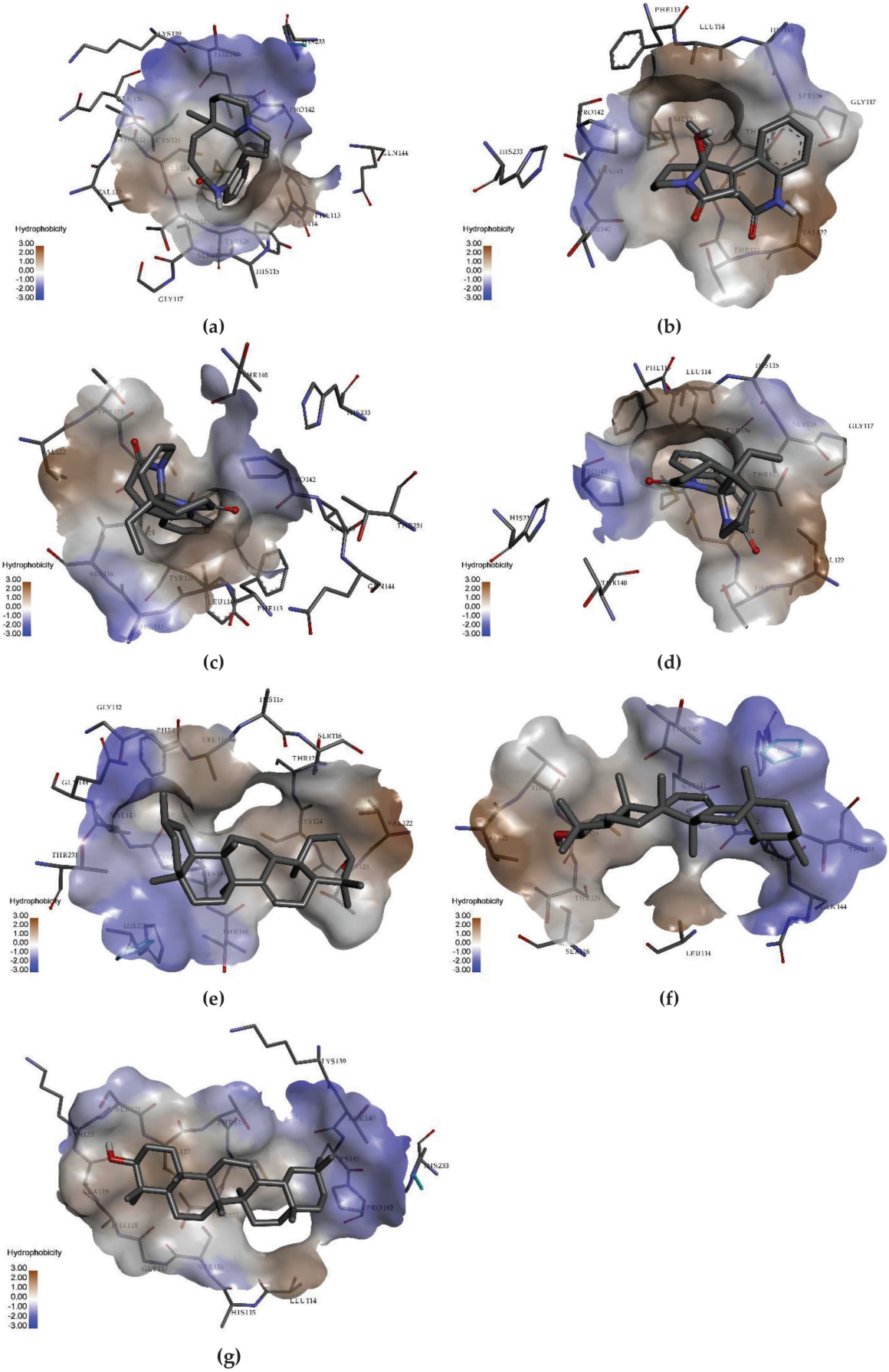

Figure 3. The 3D interactions of the compounds. **a.** Rhazinilam; **b.** Leuconolam; **c.** Leuconoxine; **d.** Dehydroleuconoxine; **e.** Baurenol; **f.** Alpha amyrin, and **g.** Beta amyrin within the p53 binding site.

upper left panel of Fig. 4. The RMSD measures the deviation of a system from its initial conformation over time, serving as an indicator of overall stability. Typically, RMSD fluctuations within the range of 0.10 to 0.30 nm are considered acceptable for globular proteins, suggesting minimal conformational changes. Baurenol showed an average RMSD of 0.29 ± 0.03 nm, while rhazinilam had an average of 0.26 ± 0.02 nm, indicating that both compounds maintained a stable binding mode to p53 throughout the simulation period. Notably, while both ligands displayed fluctuations during the initial 50 ns, they stabilized after 100 ns, with rhazinilam generally showing slightly lower RMSD values than baurenol.

The root-mean-square fluctuation (RMSF) analysis further characterizes the local flexibility of individual residues in the protein chain. RMSF highlights regions within the protein that may undergo conformational changes upon ligand binding. For both baurenol and rhazinilam, the highest fluctuations occurred around residue 275, with RMSF peaks reaching approximately 0.8 nm, indicating some flexibility in this region. However, the overall average RMSF for baurenol was 0.24 ± 0.05 nm, while for rhazinilam, it was 0.22 ± 0.04 nm, suggesting that both complexes maintained stable interactions with localized flexibility. The solvent-accessible surface area (SASA) analysis helps to understand changes in the exposure of the protein's surface to the solvent, which can reflect conformational adjustments during binding. The average SASA values for baurenol and rhazinilam were 107.8 ± 2.5 nm² and 109.2 ± 3.0 nm², respectively. The relatively stable SASA values indicate that there were no significant changes in the protein's surface area upon binding with either ligand, suggesting a consistent interaction between the ligands and p53 throughout the simulation.

Lastly, the radius of gyration analysis assesses the compactness of the protein structure during the simulation. Both baurenol and rhazinilam complexes exhibited minimal fluctuations in their radius of gyration. The average radius of gyration for baurenol was 1.69 ± 0.01 nm, while rhazinilam showed an average of 1.68 ± 0.02 nm. These values indicate that the protein maintained a stable, compact structure over the 500 ns simulation, with rhazinilam showing slightly better compactness compared to baurenol. These quantitative insights, derived from the RMSD, RMSF, SASA, and radius of gyration analyses, provide a comprehensive understanding of the stability and behavior of the baurenol and rhazinilam complexes with p53 during the MD simulation.

Hydrogen-bond interactions

The hydrogen-bond interaction analysis between baurenol and rhazinilam with p53 (PDB: 6ZNC) reveals differences in their interaction stability during the

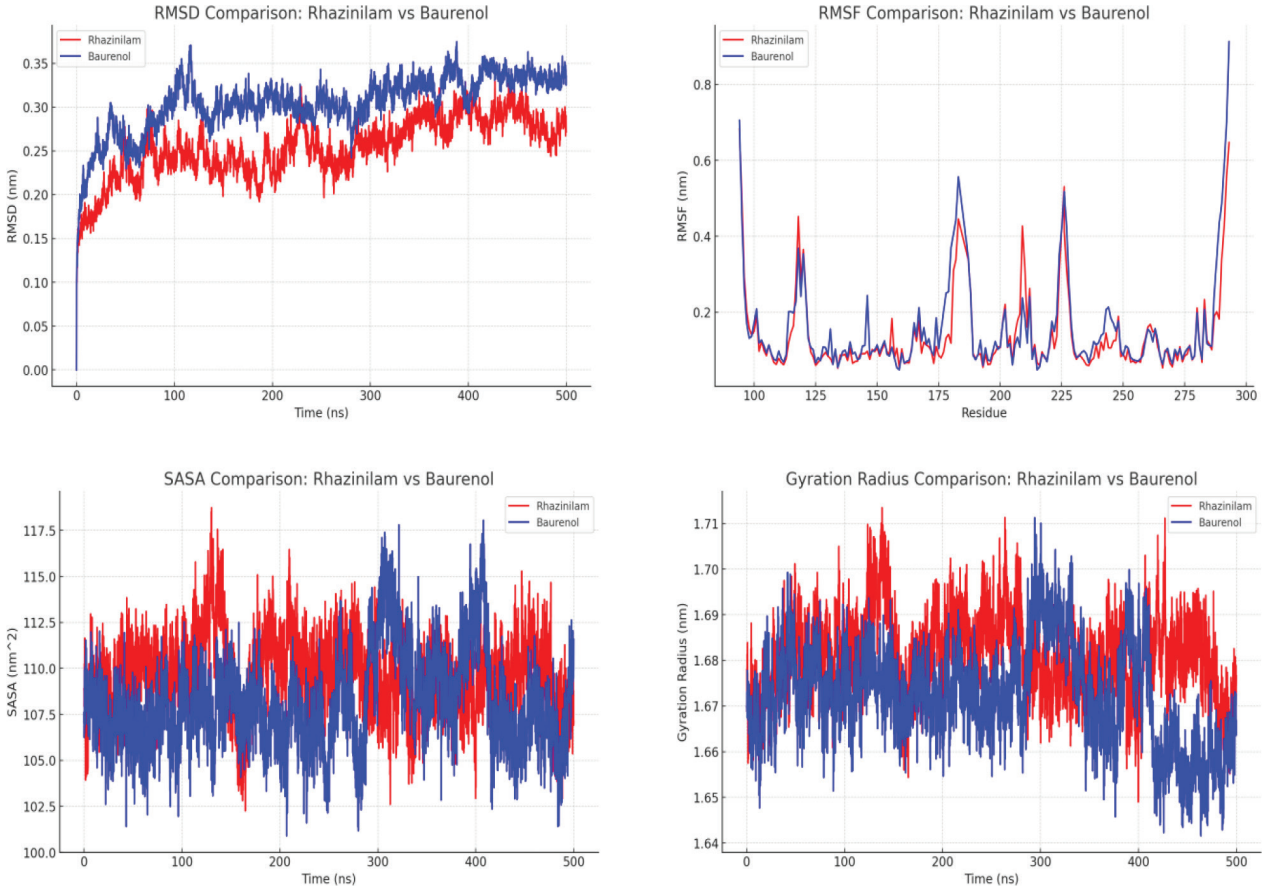

Figure 4. RMSD, RMSF, SASA, and RoG plots of protein-ligand complexes for baurenol (blue) and rhazinilam (red) with p53 (PDB: 6ZNC) during a 500 ns simulation.

500 ns simulation. As shown in Fig. 5, baurenol forms an average of approximately 0.3 hydrogen bonds, with noticeable fluctuations throughout the simulation period. It occasionally forms up to 2 hydrogen bonds, particularly at the simulation's start, but these interactions are not sustained, often dropping to zero. In contrast, rhazinilam exhibits a more consistent hydrogen-bond interaction profile. It maintains an average of about 1.2 hydrogen bonds, with several peaks reaching 2 hydrogen bonds during the first 200 ns. After this period, rhazinilam stabilizes its interaction, consistently maintaining around 1.5 to 2 hydrogen bonds until the end of the simulation. This contrast in hydrogen-bonding patterns suggests that rhazinilam has a stronger affinity for p53 compared to baurenol, as evidenced by its ability to sustain more frequent hydrogen bonds throughout the simulation. Meanwhile, baurenol's sporadic hydrogen-bond interactions indicate a less stable binding profile.

The differences in hydrogen-bond interaction patterns between baurenol and rhazinilam may reflect their varying capabilities in maintaining close contact with the binding site of the p53 protein. Rhazinilam's ability to sustain a higher number of hydrogen bonds suggests that it remains more tightly bound within the binding pocket of p53, which can lead to increased stability of the protein-ligand complex. This consistent hydrogen bonding could potentially enhance the inhibitory effect of rhazinilam on p53, making it a more effective candidate for further biological or pharmacological studies targeting this protein. In contrast, baurenol's lower average number of hydrogen bonds and the frequent interruptions in its bonding pattern indicate a more transient interaction with p53. Such variability could suggest that baurenol might not be able to maintain a strong interaction with the protein over extended periods, which might reduce its effectiveness in modulating p53's activity. These findings highlight the importance of hydrogen bonding as a key factor in assessing ligand stability and affinity in molecular dynamics simulations, and they suggest that rhazinilam may offer a more reliable interaction profile for potential therapeutic applications involving p53.

Post-MD MM-PBSA

To further assess the stability and quality of the molecular dynamics simulation, an MM-PBSA (Molecular Mechanics Poisson-Boltzmann Surface Area) analysis was performed for the baurenol and rhazinilam complexes with the p53 protein. The MM-PBSA results align with the molecular docking outcomes, providing deeper insights into the energy contributions of various interactions between the ligands and the protein. From the data in Table 4, baurenol exhibits a total binding energy of −68.568 ± 29.616 kJ/mol, while rhazinilam shows a slightly higher total binding energy of −63.538 ± 16.005 kJ/mol. The negative values indicate that both ligands bind favorably to p53, but baurenol shows a slightly stronger binding affinity based on the overall energy. Notably, the Van der Waals interactions dominate the binding energies for both ligands, with baurenol having a more negative Van der Waals energy of −96.985 ± 27.985 kJ/mol compared to −87.047 ± 18.000 kJ/mol for rhazinilam, suggesting stronger hydrophobic interactions in the baurenol complex.

Table 4. Summarized MM-PBSA analysis comparing the p53 protein (PDB: 6ZNC) in complex with baurenol and rhazinilam.

Phytochemicals	Van der Waals Energy	Electrostatic Energy	Polar Solvation Energy	SASA Energy	Total Energy
Baurenol	−96.985 ± 27.985 kJ/mol	−3.754 ± 8.294 kJ/mol	43.059 ± 16.572 kJ/mol	−10.888 ± 2.821 kJ/mol	−68.568 ± 29.616 kJ/mol
Rhazinilam	−87.047 ± 18.000 kJ/mol	−21.915 ± 20.977 kJ/mol	55.143 ± 20.484 kJ/mol	−9.718 ± 1.355 kJ/mol	−63.538 ± 16.005 kJ/mol

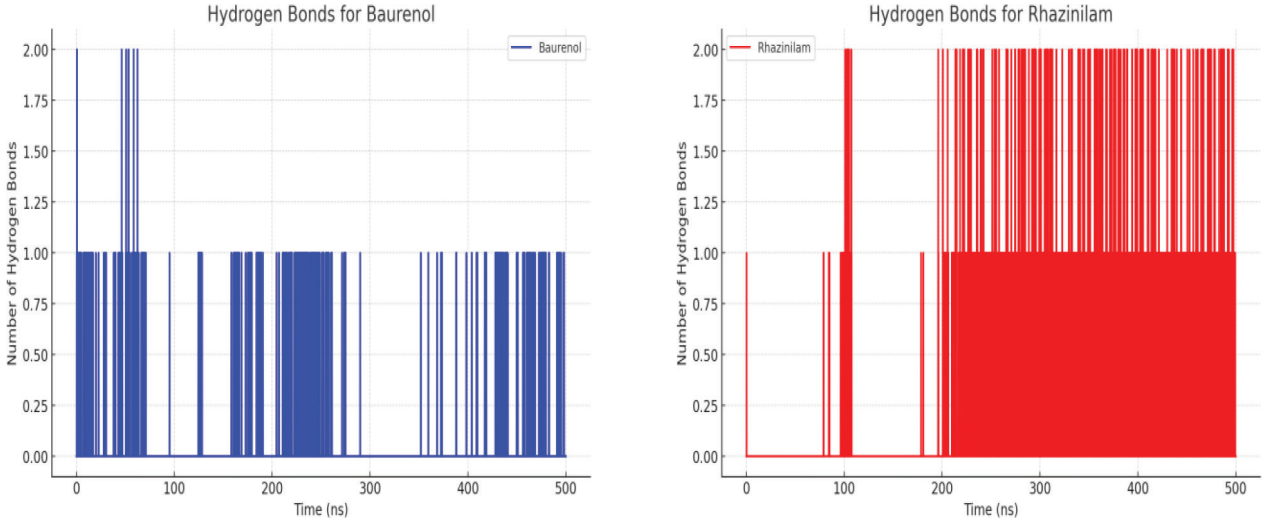

Figure 5. Plots of hydrogen-bond interactions for the protein-ligand complexes of baurenol (blue) and rhazinilam (red) with p53 (PDB: 6ZNC) throughout a 500 ns simulation.

However, rhazinilam displays a more favorable electrostatic energy of −21.915 ± 20.977 kJ/mol, in contrast to the less negative electrostatic energy of −3.754 ± 8.294 kJ/mol for baurenol. This indicates that rhazinilam forms stronger ionic interactions or hydrogen bonds with the p53 protein. Additionally, rhazinilam has a higher polar solvation energy of 55.143 ± 20.484 kJ/mol, which suggests that its binding may be more influenced by the protein's solvent environment compared to baurenol. The bar graph in Fig. 6 visualizes these energy contributions, highlighting the stronger Van der Waals interactions for baurenol and the significant electrostatic interactions for rhazinilam. Both compounds show similar contributions in terms of SASA (solvent-accessible surface area) energy, with baurenol at −10.888 ± 2.821 kJ/mol and rhazinilam at −9.718 ± 1.355 kJ/mol, suggesting comparable surface exposure in the protein-ligand complexes.

Overall, while baurenol shows a marginally stronger binding affinity due to its lower total energy, rhazinilam's stronger electrostatic interactions could provide stability advantages in different physiological conditions. This analysis provides a comprehensive understanding of the energy dynamics and interaction mechanisms between each ligand and the p53 protein. The distinct binding profiles of baurenol and rhazinilam highlight their potential for modulating p53 activity in different therapeutic contexts. Further experimental validation is required to assess how these molecular characteristics translate into actual biological outcomes, particularly in terms of their effectiveness as cancer treatments.

Discussion

Natural compounds have long been recognized for their significant role in drug discovery, especially for cancer treatment and infectious diseases. These compounds typically feature diverse chemical scaffolds, larger molecular masses, a higher number of sp3 carbon and oxygen atoms, and fewer halogen and nitrogen atoms (Lautié et al. 2020; Naeem et al. 2022). Additionally, natural products tend to have a higher number of hydrogen bond acceptors and donors, along with lower computed octanol-water partition coefficients, indicating their enrichment with bioactive components. This diversity allows natural compounds to interact with multiple biological targets, making them particularly useful in cancer therapy. The potential of these compounds to modulate critical proteins like p53, a tumor suppressor protein, is particularly appealing. P53 plays a pivotal role in regulating the cell cycle and apoptosis, and its activation in cancer cells can help inhibit tumor growth (Rahman et al. 2022). This study focused on evaluating phytochemicals derived from Sitahe (*Leuconotis eugenifolia*) as potential p53 modulators. Among the compounds tested, baurenol showed the strongest binding affinity to p53, highlighting its promising potential for cancer therapy.

Molecular dynamics (MD) simulations further provided valuable insights into the stability of the interactions between these compounds and p53. The simulations revealed that both baurenol and rhazinilam maintained stable interactions with p53 throughout the 500 ns simulation, but baurenol exhibited stronger and more consistent binding. The lower RMSD of baurenol indicated that its interaction with p53 was more stable over time compared to rhazinilam.

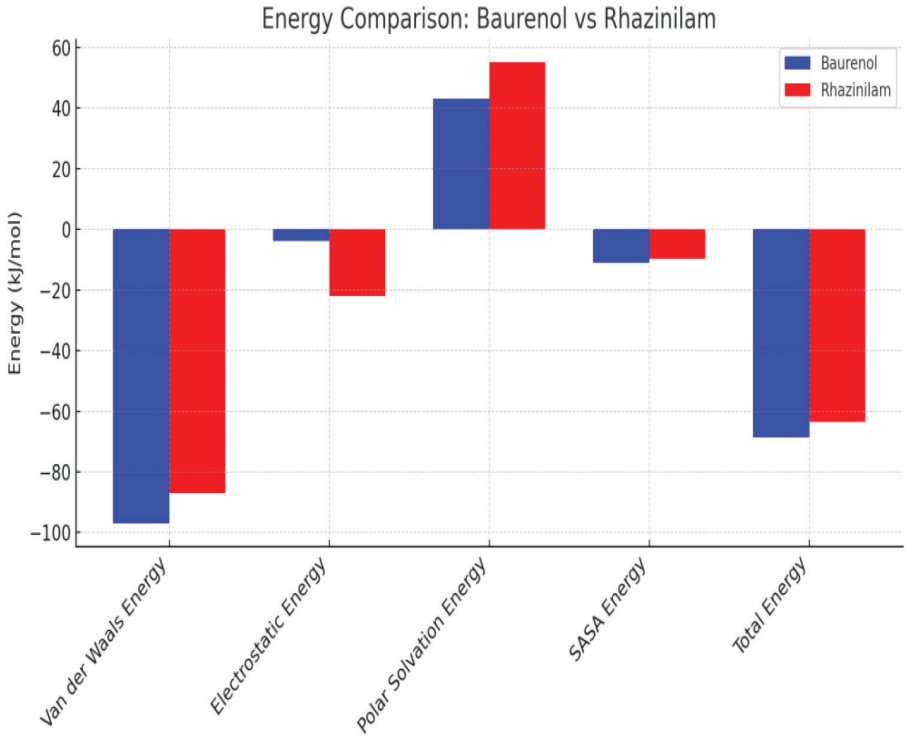

Figure 6. Comparison of energies (Van der Waals, electrostatic, polar solvation, SASA, and total) between baurenol (blue) and rhazinilam (red).

This stability is crucial for the long-term effectiveness of the compound as a therapeutic agent. The hydrophobic interactions observed in baurenol's binding to p53 further supported its ability to strongly interact with the nonpolar binding pocket of p53. While rhazinilam also showed potential, its more fluctuating binding pattern suggests that baurenol might be more effective in providing sustained therapeutic effects. These findings emphasize baurenol's potential as a leading candidate for p53-targeted cancer therapy. Additional studies are needed to validate baurenol's therapeutic potential in more complex biological systems.

In terms of binding affinity, baurenol demonstrated superior binding compared to rhazinilam, with a more favorable total binding energy in the MM-PBSA analysis. The total binding energy of baurenol (−68.568 kJ/mol) was more negative than rhazinilam's (−63.538 kJ/mol), indicating a stronger overall interaction. The dominance of Van der Waals interactions in baurenol's binding further supports its high binding affinity and stability. In contrast, while rhazinilam showed stronger electrostatic interactions, baurenol's overall binding was more stable, which is crucial for its potential as an effective cancer therapeutic. Baurenol's ability to form stable hydrogen bonds with key residues in p53, such as Thr123, further strengthens its potential to modulate p53 function effectively. This suggests that baurenol has the capacity to stabilize p53 in its active form, which is essential for promoting tumor-suppressive activity. Consequently, baurenol stands out as a promising candidate for further development in p53-targeted therapies. These results highlight baurenol's advantages in terms of both binding strength and stability.

From a bioavailability perspective, while baurenol's high lipophilicity supports membrane penetration, its low solubility in water remains a challenge for its use as a therapeutic agent. High lipophilicity allows baurenol to efficiently penetrate cell membranes, but it may limit its solubility in aqueous environments, which is crucial for optimal drug absorption (Rizkita et al. 2024). However, this property could enhance baurenol's ability to reach its target within cancer cells. As a potential radiopharmaceutical, baurenol's ability to localize in tumor cells is advantageous for targeted therapy. To address its solubility challenges, advanced drug delivery systems, such as lipid-based formulations or nanoparticle carriers, could be employed. These delivery systems could not only improve baurenol's solubility but also enhance its distribution within the body, ensuring more efficient targeting of cancer cells. Given these considerations, although solubility remains an obstacle, innovative formulation techniques could overcome this limitation and optimize its therapeutic potential (Tyagi et al. 2023). Further research into baurenol's formulation and radiolabeling for imaging purposes is crucial to maximize its effectiveness as a cancer therapy.

Finally, baurenol shows considerable promise as a p53 modulator, surpassing other compounds like rhazinilam in terms of binding affinity, interaction stability, and bioavailability potential. The compound's strong binding affinity, stability in molecular dynamics simulations, and favorable bioavailability characteristics make it a leading candidate for development as a cancer therapy (Nath et al. 2021). While challenges related to solubility remain, these can be mitigated through advanced formulation techniques, ensuring that baurenol can be used effectively in clinical settings. The next step in baurenol's development will involve in vitro and in vivo testing to validate its effectiveness in real-world biological systems. Toxicity studies will also be essential to ensure the compound's safety for long-term use (K. Vuppala 2013). With further validation, baurenol has the potential to become a breakthrough cancer therapy that is both safer and more cost-effective than current synthetic alternatives. If successful, baurenol could provide a novel treatment option for patients with cancer, offering a more natural and effective approach to modulating p53 activity.

Conclusion

This study explored the potential of several phytochemicals derived from Sitahe (*Leuconotis eugenifolia*) as modulators of the p53 protein, which plays a crucial role in cell cycle regulation and apoptosis in cancer cells. Through molecular docking, MD simulations, and MM-PBSA analysis, both compounds demonstrated favorable interactions with p53. Baurenol exhibited a higher binding affinity with a total binding energy of −68.568 kJ/mol, primarily driven by hydrophobic interactions, whereas rhazinilam showed a slightly lower affinity with a binding energy of −63.538 kJ/mol, displaying stronger electrostatic interactions and stable hydrogen bonding. The in silico ADMET screening suggested that both compounds possess favorable pharmacokinetic properties, making them promising candidates for further drug development. However, baurenol's superior binding affinity and favorable pharmacokinetic profile position it as the more promising candidate for modulating p53 and acting as a potential radioprotective agent. These findings align with previous research on natural compounds targeting p53, supporting their potential as less toxic alternatives to conventional chemotherapy. Further in vitro and in vivo studies are required to confirm their efficacy and safety as therapeutic agents targeting p53, ensuring they can effectively modulate the protein without adverse effects. If validated, baurenol could offer a new, natural approach to cancer treatment and radioprotection, contributing to more targeted and potentially safer therapeutic strategies.

Acknowledgments

The authors acknowledge the Indonesia Endowment Fund for Education (Lembaga Pengelola Dana Pendidikan, LPDP) under the Indonesian Ministry of Finance, as well as the National Research and Innovation Agency of Indonesia (BRIN), for their support and funding of the E-Rispro (Riset dan Inovasi untuk Indonesia Maju, RIIM-3) program under the grant number 12/II.7/HK/2023.

Additional information

Conflict of interest

The authors have declared that no competing interests exist.

Ethical statements

The authors declared that no clinical trials were used in the present study.
The authors declared that no experiments on humans or human tissues were performed for the present study.
The authors declared that no informed consent was obtained from the humans, donors or donors' representatives participating in the study.
The authors declared that no experiments on animals were performed for the present study.
The authors declared that no commercially available immortalised human and animal cell lines were used in the present study.

Funding

This work was supported and funding of the E-Rispro (Riset dan Inovasi untuk Indonesia Maju, RIIM-3) program under the grant number 12/II.7/HK/2023.

Author contributions

Conceptualization, D.P.P., I.K., T.M.F., B.J.T., and M.S.; methodology, D.P.P., I.K., T.M.F., and B.J.T.; software, D.P.P., I.K., T.M.F., B.J.T., T.K., and D.R.; validation, T.M.F., T.K., and H.N.E.S.; formal analysis, T.M.F., T.K., and A.M.F.; investigation, D.P.P., I.K., T.M.F., and B.J.T.; resources, T.M.F., and M.S.; data curation, I.K., T.M.F., T.K., and M.S.; writingoriginal-draft preparation, D.P.P., I.K., T.M.F., B.J.T., T.K., and M.S.; writingreview and editing, D.P.P., I.K., T.M.F., B.J.T., and M.S.; visualization, I.K., T.M.F., T.K., and M.S.; supervision, D.P.P., I.K., B.J.T., and M.S. All authors have read and agreed to the published version of the manuscript.

Author ORCIDs

Dian Pribadi Perkasa https://orcid.org/0009-0004-1637-774X
Iin Kurnia https://orcid.org/0000-0002-4599-7858
Taufik Muhammad Fakih https://orcid.org/0000-0001-7155-4412
Teja Kisnanto https://orcid.org/0000-0001-6537-7157
Dwi Ramadhani https://orcid.org/0000-0003-3018-2485
Harry Nugroho Eko Surniyantoro https://orcid.org/0000-0001-8248-7876
Boky Jeanne Tuasikal https://orcid.org/0009-0003-0423-7590
Alfian Mahardika Forentin https://orcid.org/0000-0003-2338-6172
Mukh Syaifudin https://orcid.org/0000-0003-1657-2065

Data availability

All of the data that support the findings of this study are available in the main text.

References

Abraham M, Hess B, Spoel D van der, Lindahl E (2015a) Gromacs - Reference Manual Version 2016.3. SpringerReference.

Abraham M, Hess B, Spoel D van der, Lindahl E (2015b) The GROMACS development team, GROMACS user manual. Version 5.0.7.

Abraham MJ, Murtola T, Schulz R, Páll S, Smith JC, Hess B, Lindahl E (2015c) GROMACS: High performance molecular simulations through multi-level parallelism from laptops to supercomputers. SoftwareX 1–2: 19–25. https://doi.org/10.1016/j.softx.2015.06.001

Allouche A (2012) Software news and updates gabedit — a graphical user interface for computational chemistry softwares. Journal of Computational Chemistry 32(1): 174–182. https://doi.org/10.1002/jcc.21600

Ameh-Mensah C, Duduyemi BM, Bedu-Addo K, Atta Manu E, Opoku F, Titiloye N (2021) The analysis of bcl-2 in association with p53 and Ki-67 in triple negative breast cancer and other molecular subtypes in Ghana. Journal of Oncology 2021: 054134,. https://doi.org/10.1155/2021/7054134

Bazanov DR, Pervushin NV, Savin EV, Tsymliakov MD, Maksutova AI, Savitskaya VY, Sosonyuk SE, Gracheva YA, Seliverstov MY, Lozinskaya NA, Kopeina GS (2022) Synthetic design and biological evaluation of new p53-MDM2 interaction inhibitors based on imidazoline core. Pharmaceuticals 15(4): 444. https://doi.org/10.3390/ph15040444

Boller S, Soldi C, Marques MCA, Santos EP, Cabrini DA, Pizzolatti MG, Zampronio AR, Otuki MF (2010) Anti-inflammatory effect of crude extract and isolated compounds from *Baccharis illinita* DC in acute skin inflammation. Journal of Ethnopharmacology 130(2): 262–266. https://doi.org/10.1016/j.jep.2010.05.001

Bourdon JC, Fernandes K, Murray-Zmijewski F, Liu G, Diot A, Xirodimas DP, Saville MK, Lane DP (2005) p53 isoforms can regulate p53 transcriptional activity. Genes and Development 19: 2122–2137. https://doi.org/10.1101/gad.1339905

Chen HHW, Kuo MT (2017) Improving radiotherapy in cancer treatment: Promises and challenges. Oncotarget 8: 62742–62758. https://doi.org/10.18632/oncotarget.18409

Chen S, Wu J Le, Liang Y, Tang YG, Song HX, Wu LL, Xing YF, Yan N, Li YT, Wang ZY, Xiao SJ, Lu X, Chen SJ, Lu M (2021) Arsenic trioxide rescues structural p53 mutations through a cryptic allosteric site. Cancer Cell 39: p225–239.e8. https://doi.org/10.1016/j.ccell.2020.11.013

Choi HS, Han JY, Choi YE (2020) Identification of triterpenes and functional characterization of oxidosqualene cyclases involved in triterpene biosynthesis in lettuce (*Lactuca sativa*). Plant Science 301: 110656. https://doi.org/10.1016/j.plantsci.2020.110656

Chua HM, Moshawih S, Goh HP, Ming LC, Kifli N (2023) Insights into the computer-aided drug design and discovery based on anthraquinone scaffold for cancer treatment: A protocol for systematic review. PLoS ONE 18: 0290948. https://doi.org/10.1371/journal.pone.0290948

Chung PY, Loh PLN, Neoh H min, Ramli R (2023) Alpha-amyrin as an anti-biofilm agent against methicillin-resistant and vancomycin-intermediate *Staphylococcus aureus*. Heliyon 9(7): e17892. https://doi.org/10.1016/j.heliyon.2023.e17892

Daina A, Michielin O, Zoete V (2017) SwissADME: A free web tool to evaluate pharmacokinetics, drug-likeness and medicinal chemistry friendliness of small molecules. Scientific Reports 7: 42717. https://doi.org/10.1038/srep42717

Degtjarik O, Golovenko D, Diskin-Posner Y, Abrahmsén L, Rozenberg H, Shakked Z (2021) Structural basis of reactivation of oncogenic

p53 mutants by a small molecule: methylene quinuclidinone (MQ). Nature Communications 12: 7057. https://doi.org/10.1038/s41467-021-27142-6

Delano WL (2002) The PyMOL molecular graphics system. CCP4 Newsletter on protein crystallography 40, 1–9.

Du MM, Zhu ZT, Zhang GG, Zhao YQ, Gao B, Tao XY, Liu M, Ren YH, Wang FQ, Wei DZ (2022) Engineering saccharomyces cerevisiae for hyperproduction of β-Amyrin by mitigating the inhibition effect of squalene on β-Amyrin Synthase. Journal of Agricultural and Food Chemistry 70(1): 229–237. https://doi.org/10.1021/acs.jafc.1c06712

Farshchi F, Hasanzadeh M (2023) Efficient diagnosis of cancer using biosensing of circulating tumor DNAs(ctDNA): Recent progress and challenges. Microchemical Journal 193: 109076. https://doi.org/10.1016/j.microc.2023.109076

Forli W, Halliday S, Belew R, Olson A (2012) AutoDock Version 4.2. Citeseer.

Gan CY, Low YY, Thomas NF, Kam TS (2013) Rhazinilam-leuconolam-leuconoxine alkaloids from Leuconotis griffithii. Journal of Natural Products 76(5): 957–964. https://doi.org/10.1021/np400214y

García-Ramírez J, González-Cortés LA, Miranda LD (2022) A modular synthesis of the *Rhazinilam* family of alkaloids and analogs thereof. Organic Letters 24(44): 8093–8097. https://doi.org/10.1021/acs.orglett.2c02446

Geng Q, Li Z, Lü Z, Liang G (2016) Progress in total syntheses of leuconolam-leuconoxine-mersicarpine alkaloids. Chinese Journal of Organic Chemistry 36(7): 1447–1464. https://doi.org/10.6023/cjoc201603030

Goh SH, Mohd Ali AR, Wong WH (1989) Alkaloids of *Leuconotis griffithii* and *L. eugenifolia* (Apocynaceae). Tetrahedron 45(24): 7899–7920. https://doi.org/10.1016/S0040-4020(01)85802-6

Gong L, Zhang Y, Liu C, Zhang M, Han S (2021) Application of radiosensitizers in cancer radiotherapy. International Journal of Nanomedicine 16: 1083—1102. https://doi.org/10.2147/IJN.S290438

Irish JM, Ånensen N, Hovland R, Skavland J, Børresen-Dale AL, Bruserud Ø, Nolan GP, Gjertsen BT (2007) Flt3 Y591 duplication and Bcl-2 overexpression are detected in acute myeloid leukemia cells with high levels of phosphorylated wild-type p53. Blood 109: 2589–2596. https://doi.org/10.1182/blood-2006-02-004234

K Vuppala P (2013) Importance of ADME and bioanalysis in the drug discovery. Journal of Bioequivalence & Bioavailability 05: 4. https://doi.org/10.4172/jbb.10000e31

Karami TK, Hailu S, Feng S, Graham R, Gukasyan HJ (2022) Eyes on Lipinski's Rule of Five: A New "Rule of Thumb" for Physicochemical Design Space of Ophthalmic Drugs. Journal of Ocular Pharmacology and Therapeutics 38: 1–122. https://doi.org/10.1089/jop.2021.0069

Kim R, Ferreira AJ, Beaudry CM (2019) Total synthesis of Leuconoxine, Melodinine E, and Mersicarpine through a radical translocation–cyclization cascade. Angewandte Chemie - International Edition 58(36): 12595–12598. https://doi.org/10.1002/anie.201907455

Kim S, Chen J, Cheng T, Gindulyte A, He J, He S, Li Q, Shoemaker BA, Thiessen PA, Yu B, Zaslavsky L, Zhang J, Bolton EE (2023) PubChem 2023 update. Nucleic Acids Research 51(D1): D1373–D1380. https://doi.org/10.1093/nar/gkac956

Kobayashi K, Tomita H, Shimizu M, Tanaka T, Suzui N, Miyazaki T, Hara A (2017) P53 expression as a diagnostic biomarker in ulcerative colitis-associated cancer. International Journal of Molecular Sciences 18(6): 1284. https://doi.org/10.3390/ijms18061284

Koo N, Sharma AK, Narayan S (2022) Therapeutics targeting p53-MDM2 interaction to induce cancer cell death. International Journal of Molecular Sciences 23(9): 5005. https://doi.org/10.3390/ijms23095005

Krishnaiah YS (2010) Pharmaceutical technologies for enhancing oral bioavailability of poorly soluble drugs. Journal of Bioequivalence & Bioavailability 02: 1–9. https://doi.org/10.4172/jbb.1000027

Kumari R, Kumar R, Consortium OSDD, Lynn A (2014) g _ mmpbsa - A GROMACS tool for MM-PBSA and its optimization for high-throughput binding energy calculations. Journal of Chemical Information and Modeling 54(7): 1951–1956. https://doi.org/10.1021/ci500020m

Lautié E, Russo O, Ducrot P, Boutin JA (2020) Unraveling plant natural chemical diversity for drug discovery purposes. Frontiers in Pharmacology 11: 397. https://doi.org/10.3389/fphar.2020.00397

Li Z, Geng Q, Lv Z, Pritchett BP, Baba K, Numajiri Y, Stoltz BM, Liang G (2015) Selective syntheses of leuconolam, leuconoxine, and mersicarpine alkaloids from a common intermediate through regiocontrolled cyclizations by Staudinger reactions. Organic Chemistry Frontiers 2: 236. https://doi.org/10.1039/c4qo00312h

Low YY, Hong FJ, Lim KH, Thomas NF, Kam TS (2014) Transformations of the 2,7- Seco Aspidosperma alkaloid leuconolam, structure revision of epi -leuconolam, and partial syntheses of leuconoxine and leuconodines A and F. Journal of Natural Products 77. https://doi.org/10.1021/np400922x

Lu C, Wu C, Ghoreishi D, Chen W, Wang L, Damm W, Ross GA, Dahlgren MK, Russell E, Von Bargen CD, Abel R, Friesner RA, Harder ED (2021) OPLS4: Improving force field accuracy on challenging regimes of chemical space. Journal of Chemical Theory and Computation 17(7): 4291–4300. https://doi.org/10.1021/acs.jctc.1c00302

Man KH, Law HKW, Tam SY (2023) Psychosocial needs of post-radiotherapy cancer survivors and their direct caregivers – a systematic review. Frontiers in Oncology 13: 1246844. https://doi.org/10.3389/fonc.2023.1246844

Miyamoto S, Kollman PA (1992) Settle: An analytical version of the SHAKE and RATTLE algorithm for rigid water models. Journal of Computational Chemistry 13(8): 952–962. https://doi.org/10.1002/jcc.540130805

Naeem A, Hu P, Yang M, Zhang J, Liu Y, Zhu W, Zheng Q (2022) Natural products as anticancer agents: current status and future perspectives. Molecules 27(23): 8367. https://doi.org/10.3390/molecules27238367

Nakano K, Vousden KH (2001) PUMA, a novel proapoptotic gene, is induced by p53. Molecular Cell 7(3): p683–694. https://doi.org/10.1016/S1097-2765(01)00214-3

Nath A, Kumer A, Zaben F, Khan MW (2021) Investigating the binding affinity, molecular dynamics, and ADMET properties of 2,3-dihydrobenzofuran derivatives as an inhibitor of fungi, bacteria, and virus protein. Beni-Suef University Journal of Basic and Applied Sciences 10: 36. https://doi.org/10.1186/s43088-021-00117-8

Nogueira AO, Oliveira YIS, Adjafre BL, de Moraes MEA, Aragão GF (2019) Pharmacological effects of the isomeric mixture of alpha and beta amyrin from *Protium heptaphyllum*: a literature review. Fundamental and Clinical Pharmacology 33(1): 4–12. https://doi.org/10.1111/fcp.12402

Pereira D, Lima RT, Palmeira A, Seca H, Soares J, Gomes S, Raimundo L, Maciel C, Pinto M, Sousa E, Helena Vasconcelos M, Saraiva L, Cidade H (2019) Design and synthesis of new inhibitors of p53–MDM2 interaction with a chalcone scaffold. Arabian Journal of Chemistry 12(8): 4150–4161. https://doi.org/10.1016/j.arabjc.2016.04.015

Pfaffenbach M, Gaich T (2017) The rhazinilam-leuconoxine-mersicarpine triad of monoterpenoid indole alkaloids. Alkaloids: Chemistry and Biology 77: 1–84. https://doi.org/10.1016/bs.alkal.2016.07.001

Praptiwi P, Wulansari D, Fahoni A, Harnoto N, Novita R, Alfridsyah, Agusta A (2020) Phytochemical screening, antibacterial and antioxidant assessment of Leuconotis eugenifolia leaf extract. Nusantara Bioscience 12(1): 79–85. https://doi.org/10.13057/nusbiosci/n120114

Rahman MA, Park MN, Rahman MH, Rashid MM, Islam R, Uddin MJ, Hannan MA, Kim B (2022) p53 modulation of autophagy signaling in cancer therapies: perspectives mechanism and therapeutic targets. Frontiers in Cell and Developmental Biology 10: 761080. https://doi.org/10.3389/fcell.2022.761080

Rehan M, Shafiullah (2021) The anticancer activity of oleanane-type saponin from bombax ceiba (in vitro) and theoretical investigation of signaling pathway. Malaysian Journal of Chemistry 23. https://doi.org/10.55373/mjchem.v23i1.876

Rizkita AD, Dewi SA, Fakih TM, Lee C (2024) Effectiveness of sesquiterpene derivatives from *Cinnamomum* genus in nicotine replacement therapy through blocking acetylcholine nicotinate: a computational analysis. Journal of Biomolecular Structure and Dynamics, 1–14. https://doi.org/10.1080/07391102.2024.2305315

Rogge SMJ, Vanduyfhuys L, Ghysels A, Waroquier M, Verstraelen T, Maurin G, Van Speybroeck V (2015) A comparison of barostats for the mechanical characterization of metal-organic frameworks. Journal of Chemical Theory and Computation 11(12): 5583–5597. https://doi.org/10.1021/acs.jctc.5b00748

Rühle V (2007) Berendsen and Nose-Hoover thermostats. Physics.

Shareef U, Altaf A, Ahmed M, Akhtar N, Almuhayawi MS, Al Jaouni SK, Selim S, Abdelgawad MA, Nagshabandi MK (2024) A comprehensive review of discovery and development of drugs discovered from 2020–2022. Saudi Pharmaceutical Journal 32(1): 101913. https://doi.org/10.1016/j.jsps.2023.101913

Sim KY, Mukherjee R, Toubiana MJ, Das BC (1971) Extractives from the leaves of Leuconotis eugenifolia. Phytochemistry 10(11): 2803–2806. https://doi.org/10.1016/S0031-9422(00)97283-2

Sirindil F, Weibel JM, Pale P, Blanc A (2022) Rhazinilam-leuconolam family of natural products: a half century of total synthesis. Natural Product Reports 39: 1574–1590. https://doi.org/10.1039/d2np00026a

Street W (2019) Cancer facts & figures 2019. American Cancer Society, 1–76.

Tyagi S, Pathak A, Raghavendra Rao N, Nehra S, Asthana A, Sharma V, Katyal G, Bhardwaj A, Sharma L, Prakash S, Katiyar D (2023) AI-assisted Formulation Design for Improved Drug Delivery and Bioavailability. Pakistan Heart Journal 56(3): 1–14.

Viet TD, Xuan TD, Anh LH (2021) α-Amyrin and β-Amyrin Isolated from Celastrus hindsii Leaves and Their Antioxidant, Anti-Xanthine Oxidase, and Anti-Tyrosinase Potentials. Molecules 26(23): 7248. https://doi.org/10.3390/molecules26237248

Villaseñor IM, Canlas AP, Faustino KM, Plana KG (2004) Evaluation of the bioactivity of triterpene mixture isolated from Carmona retusa (Vahl.) Masam leaves. Journal of Ethnopharmacology 92(1): 53–56. https://doi.org/10.1016/j.jep.2004.01.017

Vinod SK, Hau E (2020) Radiotherapy treatment for lung cancer: Current status and future directions. Respirology 25(S2): 61–71. https://doi.org/10.1111/resp.13870

Wang C, Greene D, Xiao L, Qi R, Luo R (2018) Recent developments and applications of the MMPBSA method. Frontiers in Molecular Biosciences 4: 87. https://doi.org/10.3389/fmolb.2017.00087

Xu Z, Wang Q, Zhu J (2013) Enantioselective total syntheses of leuconolam-leuconoxine-mersicarpine group monoterpene indole alkaloids. Journal of the American Chemical Society 135(51): 19127–19130. https://doi.org/10.1021/ja4115192

Yang Y, Bai Y, Sun S, Dai M (2014) Biosynthetically inspired divergent approach to monoterpene indole alkaloids: Total synthesis of mersicarpine, leuconodines b and d, leuconoxine, melodinine e, leuconolam, and rhazinilam. Organic Letters 16(23): 6216–6219. https://doi.org/10.1021/ol503150c

Yoon CH, Lee ES, Lim DS, Bae YS (2009) PKR, a p53 target gene, plays a crucial role in the tumor-suppressor function of p53. Proceedings of the National Academy of Sciences of the United States of America 106(19): 7852–7857. https://doi.org/10.1073/pnas.0812148106